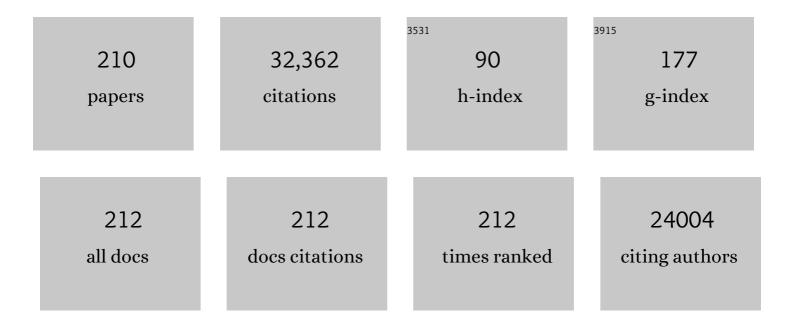
List of Publications by Year in descending order

Source: https://exaly.com/author-pdf/8373260/publications.pdf Version: 2024-02-01



WINCKELHO

#	Article	IF	CITATIONS
1	TiO2/In2S3 S-scheme photocatalyst with enhanced H2O2-production activity. Nano Research, 2023, 16, 4506-4514.	10.4	85
2	Exploring the photocatalytic conversion mechanism of gaseous formaldehyde degradation on TiO2–-OV surface. Journal of Hazardous Materials, 2022, 424, 127217.	12.4	22
3	Hierarchical Co3O4-NiO hollow dodecahedron-supported Pt for room-temperature catalytic formaldehyde decomposition. Chemical Engineering Journal, 2022, 430, 132715.	12.7	35
4	The photocatalytic NO-removal activity of g-C ₃ N ₄ significantly enhanced by the synergistic effect of Pd ⁰ nanoparticles and N vacancies. Environmental Science: Nano, 2022, 9, 742-750.	4.3	15
5	The photocatalytic •OH production activity of g-C3N4 improved by the introduction of NO. Chinese Chemical Letters, 2022, 33, 4715-4718.	9.0	10
6	Metal–Organic Frameworks for NO <i>_x</i> Adsorption and Their Applications in Separation, Sensing, Catalysis, and Biology. Small, 2022, 18, e2105484.	10.0	29
7	Highly efficient photocatalytic degradation for antibiotics and mechanism insight for Bi2S3/g-C3N4 with fast interfacial charges transfer and excellent stability. Arabian Journal of Chemistry, 2022, 15, 103689.	4.9	12
8	Polyoxometalates-doped Bi2O3–/Bi photocatalyst for highly efficient visible-light photodegradation of tetrabromobisphenol A and removal of NO. Chinese Journal of Catalysis, 2022, 43, 771-781.	14.0	17
9	In-situ synthesis of ternary heterojunctions via g-C3N4 coupling with noble-metal-free NiS and CdS with efficient visible-light-induced photocatalytic H2 evolution and mechanism insight. International Journal of Hydrogen Energy, 2022, 47, 14063-14076.	7.1	22
10	Construction and Activity of an Allâ€Organic Heterojunction Photocatalyst Based on Melem and Pyromellitic Dianhydride. ChemSusChem, 2022, 15, e202200477.	6.8	15
11	Highly Selective Photocatalytic CO ₂ Methanation with Water Vapor on Singleâ€Atom Platinumâ€Decorated Defective Carbon Nitride. Angewandte Chemie - International Edition, 2022, 61, .	13.8	60
12	Highly Selective Photocatalytic CO ₂ Methanation with Water Vapor on Singleâ€Atom Platinumâ€Decorated Defective Carbon Nitride. Angewandte Chemie, 2022, 134, .	2.0	18
13	Unraveling the Reaction Mechanism of HCHO Catalytic Oxidation on Pristine Co3O4 (110) Surface: A Theoretical Study. Catalysts, 2022, 12, 560.	3.5	1
14	Construction and Activity of an Allâ€Organic Heterojunction Photocatalyst Based on Melem and Pyromellitic Dianhydride. ChemSusChem, 2022, 15, .	6.8	2
15	Graphdiyne-based photocatalysts for solar fuel production. Green Chemistry, 2022, 24, 5739-5754.	9.0	30
16	Interfacial optimization of oxygen-vacancy-induced 1D/2D CeO2 nanotubes/g-C3N4 step-scheme heterojunction with enhanced visible-light photocatalysis and mechanism insight. Journal of Alloys and Compounds, 2022, 923, 166330.	5.5	16
17	Fabricating Z-scheme C-doped TiO ₂ /rGO nanocomposites for enhanced photocatalytic NO removal. Nanotechnology, 2022, 33, 415702.	2.6	2
18	Zn Cd1–S quantum dot with enhanced photocatalytic H2-production performance. Chinese Journal of Catalysis, 2021, 42, 15-24.	14.0	79

#	Article	IF	CITATIONS
19	Review on nickel-based adsorption materials for Congo red. Journal of Hazardous Materials, 2021, 403, 123559.	12.4	148
20	Chemical etching fabrication of uniform mesoporous Bi@Bi2O3 nanospheres with enhanced visible light-induced photocatalytic oxidation performance for NOx. Chemical Engineering Journal, 2021, 406, 126910.	12.7	51
21	Enhanced photocatalytic H2 production performance of CdS hollow spheres using C and Pt as bi-cocatalysts. Chinese Journal of Catalysis, 2021, 42, 743-752.	14.0	67
22	Design, Fabrication, and Mechanism of Nitrogenâ€Doped Grapheneâ€Based Photocatalyst. Advanced Materials, 2021, 33, e2003521.	21.0	324
23	Nearâ€Infraredâ€Responsive Photocatalysts. Small Methods, 2021, 5, e2001042.	8.6	84
24	Improved Oxygen Activation over a Carbon/Co ₃ O ₄ Nanocomposite for Efficient Catalytic Oxidation of Formaldehyde at Room Temperature. Environmental Science & Technology, 2021, 55, 4054-4063.	10.0	97
25	Enhanced solar-to-chemical energy conversion of graphitic carbon nitride by two-dimensional cocatalysts. EnergyChem, 2021, 3, 100051.	19.1	87
26	Enhanced photocatalytic activity and mechanism of CeO2 hollow spheres for tetracycline degradation. Rare Metals, 2021, 40, 2369-2380.	7.1	44
27	Enhancement in the photocatalytic H2 production activity of CdS NRs by Ag2S and NiS dual cocatalysts. Applied Catalysis B: Environmental, 2021, 288, 119994.	20.2	189
28	Tuning the strength of built-in electric field in 2D/2D g-C3N4/SnS2 and g-C3N4/ZrS2 S-scheme heterojunctions by nonmetal doping. Journal of Materiomics, 2021, 7, 988-997.	5.7	77
29	New carbon nitride close to C6N7 with superior visible light absorption for highly efficient photocatalysis. Science Bulletin, 2021, 66, 1764-1772.	9.0	25
30	g ₃ N ₄ â€Based 2D/2D Composite Heterojunction Photocatalyst. Small Structures, 2021, 2, 2100086.	12.0	127
31	Transformation of amorphous Bi2O3 to crystal Bi2O2CO3 on Bi nanospheres surface for photocatalytic NOx oxidation: Intensified hot-electron transfer and reactive oxygen species generation. Chemical Engineering Journal, 2021, 420, 129814.	12.7	35
32	Structure-Property relationship in β-keto-enamine-based covalent organic frameworks for highly efficient photocatalytic hydrogen production. Chemical Engineering Journal, 2021, 419, 129984.	12.7	56
33	Interfacial optimization of Z-scheme Ag3PO4/MoS2 nanoflower sphere heterojunction toward synergistic enhancement of visible-light-driven photocatalytic oxygen evolution and degradation of organic pollutant. Journal of Alloys and Compounds, 2021, 888, 161583.	5.5	24
34	Oxygen vacancy-dependent photocatalytic activity of well-defined Bi ₂ Sn ₂ O _{7â^²x} hollow nanocubes for NO _x removal. Environmental Science: Nano, 2021, 8, 1927-1933.	4.3	11
35	Photocatalytic Air Purification Using Functional Polymeric Carbon Nitrides. Advanced Science, 2021, 8, e2102376.	11.2	24
36	Photocatalytic reactive oxygen species generation activity of TiO ₂ improved by the modification of persistent free radicals. Environmental Science: Nano, 2021, 8, 3846-3854	4.3	11

#	Article	IF	CITATIONS
37	Enhanced photocatalytic H2-production activity of WO3/TiO2 step-scheme heterojunction by graphene modification. Chinese Journal of Catalysis, 2020, 41, 9-20.	14.0	458
38	Time-resolved characterization of non-thermal plasma-assisted photocatalytic removal of nitric oxide. Journal Physics D: Applied Physics, 2020, 53, 01LT02.	2.8	4
39	Grapheneâ€Based Materials in Planar Perovskite Solar Cells. Solar Rrl, 2020, 4, 2000502.	5.8	36
40	Construction of the 1D Covalent Organic Framework/2D g-C ₃ N ₄ Heterojunction with High Apparent Quantum Efficiency at 500 nm. ACS Applied Materials & Interfaces, 2020, 12, 51555-51562.	8.0	50
41	Room-temperature formaldehyde catalytic decomposition. Environmental Science: Nano, 2020, 7, 3655-3709.	4.3	64
42	g ₃ N ₄ /TiO ₂ Composite Film in the Fabrication of a Photocatalytic Airâ€Purifying Pavements. Solar Rrl, 2020, 4, 2000170.	5.8	23
43	A Review of Co3O4-based Catalysts for Formaldehyde Oxidation at Low Temperature: Effect Parameters and Reaction Mechanism. Aerosol Science and Engineering, 2020, 4, 147-168.	1.9	16
44	Photocatalytic CO ₂ reduction of C/ZnO nanofibers enhanced by an Ni-NiS cocatalyst. Nanoscale, 2020, 12, 7206-7213.	5.6	80
45	Lowâ€Temperatureâ€Processed Zr/F Coâ€Doped SnO ₂ Electron Transport Layer for Highâ€Efficiency Planar Perovskite Solar Cells. Solar Rrl, 2020, 4, 2000090.	5.8	42
46	Novel N/Carbon Quantum Dot Modified MIL-125(Ti) Composite for Enhanced Visible-Light Photocatalytic Removal of NO. Industrial & Engineering Chemistry Research, 2020, 59, 6470-6478.	3.7	26
47	Oxygen vacancy–engineered Î′-MnO /activated carbon for room-temperature catalytic oxidation of formaldehyde. Applied Catalysis B: Environmental, 2020, 278, 119294.	20.2	87
48	Graphdiyne: A Brilliant Hole Accumulator for Stable and Efficient Planar Perovskite Solar Cells. Small, 2020, 16, e1907290.	10.0	45
49	Synthesis and characterization of Bi-BiPO4 nanocomposites as plasmonic photocatalysts for oxidative NO removal. Applied Surface Science, 2020, 513, 145775.	6.1	32
50	C3N4 with engineered three coordinated (N3C) nitrogen vacancy boosts the production of 1O2 for Efficient and stable NO photo-oxidation. Chemical Engineering Journal, 2020, 389, 124421.	12.7	60
51	Reasonable design of Cu2MoS4 heterophase junction for highly efficient photocatalysis. Journal of Alloys and Compounds, 2020, 826, 154076.	5.5	18
52	NiFe-LDH nanosheet/carbon fiber nanocomposite with enhanced anionic dye adsorption performance. Applied Surface Science, 2020, 511, 145570.	6.1	112
53	2D/2D/0D TiO2/C3N4/Ti3C2 MXene composite S-scheme photocatalyst with enhanced CO2 reduction activity. Applied Catalysis B: Environmental, 2020, 272, 119006.	20.2	604
54	Organophosphate flame retardants and bisphenol A in children's urine in Hong Kong: has the burden been underestimated?. Ecotoxicology and Environmental Safety, 2019, 183, 109502.	6.0	15

#	Article	IF	CITATIONS
55	Active Complexes on Engineered Crystal Facets of MnO _x –CeO ₂ and Scale-Up Demonstration on an Air Cleaner for Indoor Formaldehyde Removal. Environmental Science & Technology, 2019, 53, 10906-10916.	10.0	36
56	Urea and Melamine Formaldehyde Resin-Derived Tubular g-C ₃ N ₄ with Highly Efficient Photocatalytic Performance. ACS Applied Materials & Interfaces, 2019, 11, 27934-27943.	8.0	54
57	Two-dimensional polyimide heterojunctions for the efficient removal of environmental pollutants under visible-light irradiation. Physical Chemistry Chemical Physics, 2019, 21, 17163-17169.	2.8	8
58	Ultra violet filters in the urine of preschool children and drinking water. Environment International, 2019, 133, 105246.	10.0	20
59	S‣cheme Heterojunction TiO ₂ /CdS Nanocomposite Nanofiber as H ₂ â€Production Photocatalyst. ChemCatChem, 2019, 11, 6301-6309.	3.7	286
60	Hierarchical porous Ni/Co-LDH hollow dodecahedron with excellent adsorption property for Congo red and Cr(VI) ions. Applied Surface Science, 2019, 478, 981-990.	6.1	204
61	Effects of H2O2 generation over visible light-responsive Bi/Bi2O2â^'CO3 nanosheets on their photocatalytic NO removal performance. Chemical Engineering Journal, 2019, 363, 374-382.	12.7	56
62	Photocatalytic H2 evolution on graphdiyne/g-C3N4 hybrid nanocomposites. Applied Catalysis B: Environmental, 2019, 255, 117770.	20.2	284
63	Constructing Z-scheme SnO ₂ /N-doped carbon quantum dots/ZnSn(OH) ₆ nanohybrids with high redox ability for NO <i>x</i> removal under VIS-NIR light. Journal of Materials Chemistry A, 2019, 7, 15782-15793.	10.3	60
64	In Situ Intermediates Determination and Cytotoxicological Assessment in Catalytic Oxidation of Formaldehyde: Implications for Catalyst Design and Selectivity Enhancement under Ambient Conditions. Environmental Science & Technology, 2019, 53, 5230-5240.	10.0	10
65	Engineering of reduced graphene oxide on nanosheet–g-C3N4/perylene imide heterojunction for enhanced photocatalytic redox performance. Applied Catalysis B: Environmental, 2019, 250, 42-51.	20.2	58
66	3D hierarchical graphene oxide-NiFe LDH composite with enhanced adsorption affinity to Congo red, methyl orange and Cr(VI) ions. Journal of Hazardous Materials, 2019, 369, 214-225.	12.4	329
67	Roles of N-Vacancies over Porous g-C ₃ N ₄ Microtubes during Photocatalytic NO <i>_x</i> Removal. ACS Applied Materials & Interfaces, 2019, 11, 10651-10662.	8.0	210
68	Enhanced Photocatalytic Activity and Selectivity for CO ₂ Reduction over a TiO ₂ Nanofibre Mat Using Ag and MgO as Bi ocatalyst. ChemCatChem, 2019, 11, 465-472.	3.7	81
69	Protonated g-C3N4/Ti3+ self-doped TiO2 nanocomposite films: Room-temperature preparation, hydrophilicity, and application for photocatalytic NO removal. Applied Catalysis B: Environmental, 2019, 240, 122-131.	20.2	122
70	Hierarchical porous Al2O3@ZnO core-shell microfibres with excellent adsorption affinity for Congo red molecule. Applied Surface Science, 2019, 473, 251-260.	6.1	61
71	Review on Metal Sulphideâ€based Zâ€scheme Photocatalysts. ChemCatChem, 2019, 11, 1394-1411.	3.7	439
72	Hierarchically CdS–Ag2S nanocomposites for efficient photocatalytic H2 production. Applied Surface Science, 2019, 470, 196-204.	6.1	189

#	Article	IF	CITATIONS
73	Highly enhanced visible-light photocatalytic NO x purification and conversion pathway on self-structurally modified g-C 3 N 4 nanosheets. Science Bulletin, 2018, 63, 609-620.	9.0	72
74	Synthesis of a Bi2O2CO3/ZnFe2O4 heterojunction with enhanced photocatalytic activity for visible light irradiation-induced NO removal. Applied Catalysis B: Environmental, 2018, 234, 70-78.	20.2	167
75	Workability and mechanical properties of alkali-activated fly ash-slag concrete cured at ambient temperature. Construction and Building Materials, 2018, 172, 476-487.	7.2	305
76	Phosphorus flame retardants and Bisphenol A in indoor dust and PM2.5 in kindergartens and primary schools in Hong Kong. Environmental Pollution, 2018, 235, 365-371.	7.5	59
77	Biocompatible FeOOH-Carbon quantum dots nanocomposites for gaseous NO removal under visible light: Improved charge separation and High selectivity. Journal of Hazardous Materials, 2018, 354, 54-62.	12.4	126
78	Unraveling the mechanisms of room-temperature catalytic degradation of indoor formaldehyde and its biocompatibility on colloidal TiO ₂ -supported MnO _x –CeO ₂ . Environmental Science: Nano, 2018, 5, 1130-1139.	4.3	21
79	Carbon vacancy-induced enhancement of the visible light-driven photocatalytic oxidation of NO over g-C 3 N 4 nanosheets. Applied Surface Science, 2018, 430, 380-389.	6.1	189
80	<i>In situ</i> g-C ₃ N ₄ self-sacrificial synthesis of a g-C ₃ N ₄ /LaCO ₃ OH heterostructure with strong interfacial charge transfer and separation for photocatalytic NO removal. Journal of Materials Chemistry A, 2018, 6, 972-981.	10.3	54
81	Graphene-induced formation of visible-light-responsive SnO2-Zn2SnO4 Z-scheme photocatalyst with surface vacancy for the enhanced photoreactivity towards NO and acetone oxidation. Chemical Engineering Journal, 2018, 336, 200-210.	12.7	79
82	Direct Z-scheme porous g-C3N4/BiOI heterojunction for enhanced visible-light photocatalytic activity. Journal of Alloys and Compounds, 2018, 766, 841-850.	5.5	115
83	Synthesis of SrFexTi1-xO3-l´ nanocubes with tunable oxygen vacancies for selective and efficient photocatalytic NO oxidation. Applied Catalysis B: Environmental, 2018, 239, 1-9.	20.2	46
84	Review on nanoscale Bi-based photocatalysts. Nanoscale Horizons, 2018, 3, 464-504.	8.0	421
85	Self-assembly synthesis of boron-doped graphitic carbon nitride hollow tubes for enhanced photocatalytic NOx removal under visible light. Applied Catalysis B: Environmental, 2018, 239, 352-361.	20.2	154
86	Fabrication of TiO 2 nanorod assembly grafted rGO (rGO@TiO 2 -NR) hybridized flake-like photocatalyst. Applied Surface Science, 2017, 391, 218-227.	6.1	81
87	Environment-Friendly Carbon Quantum Dots/ZnFe ₂ O ₄ Photocatalysts: Characterization, Biocompatibility, and Mechanisms for NO Removal. Environmental Science & Technology, 2017, 51, 2924-2933.	10.0	260
88	Peroxymonosulfate activated by amorphous particulate MnO2 for mineralization of benzene gas: Redox reaction, weighting analysis, and numerical modelling. Chemical Engineering Journal, 2017, 316, 61-69.	12.7	14
89	Effect of mesoporous g-C3N4 substrate on catalytic oxidation of CO over Co3O4. Applied Surface Science, 2017, 401, 333-340.	6.1	63
90	Enhanced photocatalytic removal of NO over titania/hydroxyapatite (TiO ₂ /HAp) composites with improved adsorption and charge mobility ability. RSC Advances, 2017, 7, 24683-24689.	3.6	52

#	Article	IF	CITATIONS
91	Enhanced visible-light photo-oxidation of nitric oxide using bismuth-coupled graphitic carbon nitride composite heterostructures. Chinese Journal of Catalysis, 2017, 38, 321-329.	14.0	95
92	Improving photoanodes to obtain highly efficient dye-sensitized solar cells: a brief review. Materials Horizons, 2017, 4, 319-344.	12.2	152
93	Controllable Synthesis of Core–Shell Bi@Amorphous Bi ₂ O ₃ Nanospheres with Tunable Optical and Photocatalytic Activity for NO Removal. Industrial & Engineering Chemistry Research, 2017, 56, 10251-10258.	3.7	66
94	Veterinary antibiotics in food, drinking water, and the urine of preschool children in Hong Kong. Environment International, 2017, 108, 246-252.	10.0	155
95	Review on the improvement of the photocatalytic and antibacterial activities of ZnO. Journal of Alloys and Compounds, 2017, 727, 792-820.	5.5	884
96	Three-Dimensional Bi \$\$_{5}\$\$ 5 O \$\$_{7}\$\$ 7 I Photocatalysts for Efficient Removal of NO in Air Under Visible Light. Aerosol Science and Engineering, 2017, 1, 33-40.	1.9	6
97	Fabrication and photocatalytic activity enhanced mechanism of direct Z-scheme g-C 3 N 4 /Ag 2 WO 4 photocatalyst. Applied Surface Science, 2017, 391, 175-183.	6.1	601
98	Hybridization of rutile TiO2 (rTiO2) with g-C3N4 quantum dots (CN QDs): An efficient visible-light-driven Z-scheme hybridized photocatalyst. Applied Catalysis B: Environmental, 2017, 202, 611-619.	20.2	296
99	Perovskite LaFeO3-SrTiO3 composite for synergistically enhanced NO removal under visible light excitation. Applied Catalysis B: Environmental, 2017, 204, 346-357.	20.2	127
100	Highly photoreactive TiO2 hollow microspheres with super thermal stability for acetone oxidation. Chinese Journal of Catalysis, 2017, 38, 2085-2093.	14.0	42
101	A review on TiO2-based Z-scheme photocatalysts. Chinese Journal of Catalysis, 2017, 38, 1936-1955.	14.0	511
102	Facile Synthesis of ZnxCd1-xS Solid Solution Microspheres through Ultrasonic Spray Pyrolysis for Improved Photocatalytic Activity. Journal of Nanomaterials, 2017, 2017, 1-8.	2.7	2
103	Mechanism of NO Photocatalytic Oxidation on g-C3N4 Was Changed by Pd-QDs Modification. Molecules, 2016, 21, 36.	3.8	22
104	Recent Development of Plasmonic Resonance-Based Photocatalysis and Photovoltaics for Solar Utilization. Molecules, 2016, 21, 180.	3.8	54
105	Thiourea-Modified TiO2 Nanorods with Enhanced Photocatalytic Activity. Molecules, 2016, 21, 181.	3.8	24
106	Insight into the Photocatalytic Removal of NO in Air over Nanocrystalline Bi ₂ Sn ₂ O ₇ under Simulated Solar Light. Industrial & Engineering Chemistry Research, 2016, 55, 10609-10617.	3.7	34
107	In situ Fabrication of $\hat{1}\pm$ -Bi2O3/(BiO)2CO3 Nanoplate Heterojunctions with Tunable Optical Property and Photocatalytic Activity. Scientific Reports, 2016, 6, 23435.	3.3	65
108	Fabrication and enhanced CO2 reduction performance of N-self-doped TiO2 microsheet photocatalyst by bi-cocatalyst modification. Journal of CO2 Utilization, 2016, 16, 442-449.	6.8	99

#	Article	IF	CITATIONS
109	Plasmonic Bi/ZnWO ₄ Microspheres with Improved Photocatalytic Activity on NO Removal under Visible Light. ACS Sustainable Chemistry and Engineering, 2016, 4, 6912-6920.	6.7	88
110	Fabrication of Bi2O2CO3/g-C3N4 heterojunctions for efficiently photocatalytic NO in air removal: In-situ self-sacrificial synthesis, characterizations and mechanistic study. Applied Catalysis B: Environmental, 2016, 199, 123-133.	20.2	214
111	Photocatalytic selective oxidation of phenol to produce dihydroxybenzenes in a TiO 2 /UV system: Hydroxyl radical versus hole. Applied Catalysis B: Environmental, 2016, 199, 405-411.	20.2	95
112	Hierarchically porous NiO–Al ₂ O ₃ nanocomposite with enhanced Congo red adsorption in water. RSC Advances, 2016, 6, 10272-10279.	3.6	72
113	Visible-Light-Active Plasmonic Ag–SrTiO ₃ Nanocomposites for the Degradation of NO in Air with High Selectivity. ACS Applied Materials & Interfaces, 2016, 8, 4165-4174.	8.0	132
114	Simultaneous excitation of PdCl2 hybrid mesoporous g-C3N4 molecular/solid-state photocatalysts for enhancing the visible-light-induced oxidative removal of nitrogen oxides. Applied Catalysis B: Environmental, 2016, 184, 174-181.	20.2	39
115	Hierarchical porous ZnWO4 microspheres synthesized by ultrasonic spray pyrolysis: Characterization, mechanistic and photocatalytic NO removal studies. Applied Catalysis A: General, 2016, 515, 170-178.	4.3	59
116	Distribution of bacteria in inhalable particles and its implications for health risks in kindergarten children in Hong Kong. Atmospheric Environment, 2016, 128, 268-275.	4.1	20
117	Halogen poisoning effect of Pt-TiO2 for formaldehyde catalytic oxidation performance at room temperature. Applied Surface Science, 2016, 364, 808-814.	6.1	124
118	Hierarchical NiO–SiO2 composite hollow microspheres with enhanced adsorption affinity towards Congo red in water. Journal of Colloid and Interface Science, 2016, 466, 238-246.	9.4	133
119	Self doping promoted photocatalytic removal of no under visible light with bi2moo6: Indispensable role of superoxide ions. Applied Catalysis B: Environmental, 2016, 182, 316-325.	20.2	157
120	High-surface area mesoporous Pt/TiO 2 hollow chains for efficient formaldehyde decomposition at ambient temperature. Journal of Hazardous Materials, 2016, 301, 522-530.	12.4	162
121	Performance and mechanism of visible-light-induced plasmonic photocatalytic purification of NO with Ag/AgX. Chinese Science Bulletin, 2016, 61, 3482-3489.	0.7	2
122	Mass-Controlled Direct Synthesis of Graphene-like Carbon Nitride Nanosheets with Exceptional High Visible Light Activity. Less is Better. Scientific Reports, 2015, 5, 14643.	3.3	71
123	Hierarchical Pt/NiO Hollow Microspheres with Enhanced Catalytic Performance. ChemNanoMat, 2015, 1, 58-67.	2.8	78
124	A Hierarchical Z-Scheme CdS-WO ₃ Photocatalyst with Enhanced CO ₂ Reduction Activity. Small, 2015, 11, 5262-5271.	10.0	682
125	Nanocasting of Periodic Mesoporous Materials as an Effective Strategy to Prepare Mixed Phases of Titania. Molecules, 2015, 20, 21881-21895.	3.8	8
126	Photocatalytic NO removal on BiOI surface: The change from nonselective oxidation to selective oxidation to selective oxidation. Applied Catalysis B: Environmental, 2015, 168-169, 490-496.	20.2	88

#	Article	IF	CITATIONS
127	Efficient photocatalytic degradation of NO by ceramic foam air filters coated with mesoporous TiO2 thin films. Chinese Journal of Catalysis, 2015, 36, 2109-2118.	14.0	16
128	Enhanced catalytic activity of hierarchically macro-/mesoporous Pt/TiO ₂ toward room-temperature decomposition of formaldehyde. Catalysis Science and Technology, 2015, 5, 2366-2377.	4.1	86
129	Facile fabrication of porous Cr-doped SrTiO ₃ nanotubes by electrospinning and their enhanced visible-light-driven photocatalytic properties. Journal of Materials Chemistry A, 2015, 3, 3935-3943.	10.3	62
130	New insights into how RGO influences the photocatalytic performance of BiOIO3/RGO nanocomposites under visible and UV irradiation. Journal of Colloid and Interface Science, 2015, 447, 16-24.	9.4	71
131	Synthesis and adsorption performance of Mg(OH)2 hexagonal nanosheet–graphene oxide composites. Applied Surface Science, 2015, 332, 121-129.	6.1	121
132	Improving g-C3N4 photocatalysis for NOx removal by Ag nanoparticles decoration. Applied Surface Science, 2015, 358, 356-362.	6.1	101
133	Sulfur-doped g-C3N4 with enhanced photocatalytic CO2-reduction performance. Applied Catalysis B: Environmental, 2015, 176-177, 44-52.	20.2	919
134	Enhanced visible light photocatalytic activity and oxidation ability of porous graphene-like g-C3N4 nanosheets via thermal exfoliation. Applied Surface Science, 2015, 358, 393-403.	6.1	378
135	Enhanced visible-light-driven photocatalytic removal of NO: Effect on layer distortion on g-C3N4 by H2 heating. Applied Catalysis B: Environmental, 2015, 179, 106-112.	20.2	131
136	Copolymerization with 2,4,6-Triaminopyrimidine for the Rolling-up the Layer Structure, Tunable Electronic Properties, and Photocatalysis of g-C ₃ N ₄ . ACS Applied Materials & Interfaces, 2015, 7, 5497-5505.	8.0	264
137	Facile synthesis of porous graphene-like carbon nitride (C6N9H3) with excellent photocatalytic activity for NO removal. Applied Catalysis B: Environmental, 2015, 174-175, 477-485.	20.2	159
138	Isoelectric point and adsorption activity of porous g-C3N4. Applied Surface Science, 2015, 344, 188-195.	6.1	753
139	The role and synergistic effect of the light irradiation and H2O2 in photocatalytic inactivation of Escherichia coli. Journal of Photochemistry and Photobiology B: Biology, 2015, 149, 164-171.	3.8	22
140	Controllable synthesis of phosphate-modified BiPO ₄ nanorods with high photocatalytic activity: surface hydroxyl groups concentrations effects. RSC Advances, 2015, 5, 99712-99721.	3.6	24
141	Graphene-Based Photocatalysts for CO ₂ Reduction to Solar Fuel. Journal of Physical Chemistry Letters, 2015, 6, 4244-4251.	4.6	368
142	Selective photocatalytic N ₂ fixation dependent on g-C ₃ N ₄ induced by nitrogen vacancies. Journal of Materials Chemistry A, 2015, 3, 23435-23441.	10.3	495
143	Photocatalytic activity of Ag ₂ MO ₄ (M = Cr, Mo, W) photocatalysts. Journal of Materials Chemistry A, 2015, 3, 20153-20166.	10.3	152
144	Water-assisted production of honeycomb-like g-C ₃ N ₄ with ultralong carrier lifetime and outstanding photocatalytic activity. Nanoscale, 2015, 7, 2471-2479.	5.6	328

#	Article	IF	CITATIONS
145	The mechanism of enhanced visible light photocatalysis with micro-structurally optimized and graphene oxide coupled(BiO) ₂ CO ₃ . Chinese Science Bulletin, 2015, 60, 1915-1923.	0.7	3

146 石墨åž‹C<sub>3</sub>N<sub>4</sub>在泡沫é™¶ç"·è¡¨é¢çš"原ä¼2èŶè¼2½åŠå•è§å..0‰å,¬åŒ⊋空æ°"å

147	Nanomaterials for Environmental Applications. Journal of Nanomaterials, 2014, 2014, 1-4.	2.7	24
148	Hydrothermal fabrication of N-doped (BiO)2CO3: Structural and morphological influence on the visible light photocatalytic activity. Applied Surface Science, 2014, 319, 256-264.	6.1	27
149	Growth of BiOBr nanosheets on C3N4 nanosheets to construct two-dimensional nanojunctions with enhanced photoreactivity for NO removal. Journal of Colloid and Interface Science, 2014, 418, 317-323.	9.4	136
150	Noble Metal-Like Behavior of Plasmonic Bi Particles as a Cocatalyst Deposited on (BiO) ₂ CO ₃ Microspheres for Efficient Visible Light Photocatalysis. ACS Catalysis, 2014, 4, 4341-4350.	11.2	441
151	Synthesis of mesoporous polymeric carbon nitride exhibiting enhanced and durable visible light photocatalytic performance. Science Bulletin, 2014, 59, 688-698.	1.7	33
152	Metal-free disinfection effects induced by graphitic carbon nitride polymers under visible light illumination. Chemical Communications, 2014, 50, 4338.	4.1	187
153	Immobilization of Polymeric g-C ₃ N ₄ on Structured Ceramic Foam for Efficient Visible Light Photocatalytic Air Purification with Real Indoor Illumination. Environmental Science & Technology, 2014, 48, 10345-10353.	10.0	436
154	Enhancing the photocatalytic activity of bulk g-C3N4 by introducing mesoporous structure and hybridizing with graphene. Journal of Colloid and Interface Science, 2014, 436, 29-36.	9.4	92
155	Engineering the nanoarchitecture and texture of polymeric carbon nitride semiconductor for enhanced visible light photocatalytic activity. Journal of Colloid and Interface Science, 2013, 401, 70-79.	9.4	358
155 156	enhanced visible light photocatalytic activity. Journal of Colloid and Interface Science, 2013, 401,	9.4 8.0	358 1,102
	enhanced visible light photocatalytic activity. Journal of Colloid and Interface Science, 2013, 401, 70-79. In Situ Construction of g-C ₃ N ₄ /g-C ₃ N ₄ Metal-Free Heterojunction for Enhanced Visible-Light Photocatalysis. ACS Applied Materials & amp; Interfaces,		
156	enhanced visible light photocatalytic activity. Journal of Colloid and Interface Science, 2013, 401, 70-79. In Situ Construction of g-C ₃ N ₄ /g-C ₃ N ₄ Metal-Free Heterojunction for Enhanced Visible-Light Photocatalysis. ACS Applied Materials & amp; Interfaces, 2013, 5, 11392-11401. CdIn2S4 microsphere as an efficient visible-light-driven photocatalyst for bacterial inactivation: Synthesis, characterizations and photocatalytic inactivation mechanisms. Applied Catalysis B:	8.0	1,102
156 157	 enhanced visible light photocatalytic activity. Journal of Colloid and Interface Science, 2013, 401, 70-79. In Situ Construction of g-C₃N₄/g-C₃N₄ Metal-Free Heterojunction for Enhanced Visible-Light Photocatalysis. ACS Applied Materials & amp; Interfaces, 2013, 5, 11392-11401. CdIn2S4 microsphere as an efficient visible-light-driven photocatalyst for bacterial inactivation: Synthesis, characterizations and photocatalytic inactivation mechanisms. Applied Catalysis B: Environmental, 2013, 129, 482-490. Synthesis of flower-like, pinon-like and faceted nanoplates (BiO)2CO3 micro/nanostructures with 	8.0 20.2	1,102 170
156 157 158	 enhanced visible light photocatalytic activity. Journal of Colloid and Interface Science, 2013, 401, 70-79. In Situ Construction of g-C (sub>3 (sub>N (sub>4 (sub>)g-C (sub>3 (sub>N (sub>4 (sub> Metal-Free Heterojunction for Enhanced Visible-Light Photocatalysis. ACS Applied Materials & amp; Interfaces, 2013, 5, 11392-11401. CdIn2S4 microsphere as an efficient visible-light-driven photocatalyst for bacterial inactivation: Synthesis, characterizations and photocatalytic inactivation mechanisms. Applied Catalysis B: Environmental, 2013, 129, 482-490. Synthesis of flower-like, pinon-like and faceted nanoplates (BiO)2CO3 micro/nanostructures with morphology-dependent photocatalytic activity. Materials Chemistry and Physics, 2013, 142, 381-386. (NH4)2CO3 mediated hydrothermal synthesis of N-doped (BiO)2CO3 hollow nanoplates microspheres as high-performance and durable visible light photocatalyst for air cleaning. Chemical Engineering Journal, 2013, 214, 198-207. Coreâ€"shell Feâ€"Fe2O3 nanostructures as effective persulfate activator for degradation of methyl orange. Separation and Purification Technology, 2013, 108, 159-165. 	8.0 20.2 4.0	1,102 170 17
156 157 158 159	 enhanced visible light photocatalytic activity. Journal of Colloid and Interface Science, 2013, 401, 70-79. In Situ Construction of g-C₃N₄/g-C₃N₄/Metal-Free Heterojunction for Enhanced Visible-Light Photocatalysis. ACS Applied Materials & amp; Interfaces, 2013, 5, 11392-11401. Cdln2S4 microsphere as an efficient visible-light-driven photocatalyst for bacterial inactivation: Synthesis, characterizations and photocatalytic inactivation mechanisms. Applied Catalysis B: Environmental, 2013, 129, 482-490. Synthesis of flower-like, pinon-like and faceted nanoplates (BiO)2CO3 micro/nanostructures with morphology-dependent photocatalytic activity. Materials Chemistry and Physics, 2013, 142, 381-386. (NH4)2CO3 mediated hydrothermal synthesis of N-doped (BiO)2CO3 hollow nanoplates microspheres as high-performance and durable visible light photocatalyst for air cleaning. Chemical Engineering Journal, 2013, 214, 198-207. Coreâ€"shell Feâ€"Fe2O3 nanostructures as effective persulfate activator for degradation of methyl 	8.0 20.2 4.0 12.7	1,102 170 17 83

#	Article	IF	CITATIONS
163	Controlled synthesis, growth mechanism and highly efficient solar photocatalysis of nitrogen-doped bismuth subcarbonate hierarchical nanosheets architectures. Dalton Transactions, 2012, 41, 8270.	3.3	65
164	One-pot template-free synthesis, growth mechanism and enhanced photocatalytic activity of monodisperse (BiO)2CO3 hierarchical hollow microspheres self-assembled with single-crystalline nanosheets. CrystEngComm, 2012, 14, 3534.	2.6	79
165	A stable single-crystal Bi3NbO7 nanoplates superstructure for effective visible-light-driven photocatalytic removal of nitric oxide. Applied Surface Science, 2012, 263, 266-272.	6.1	28
166	Novel in Situ N-Doped (BiO) ₂ CO ₃ Hierarchical Microspheres Self-Assembled by Nanosheets as Efficient and Durable Visible Light Driven Photocatalyst. Langmuir, 2012, 28, 766-773.	3.5	218
167	Fabrication of Bi-Doped <mml:math xmlns:mml="http://www.w3.org/1998/Math/MathML"><mml:mrow><mml:mi>T</mml:mi><mml:msub><mml:m with Ultrasonic Spray Pyrolysis and Investigation of Their Visible-Light Photocatalytic Properties. Journal of Nanotechnology, 2012, 2012, 1-7.</mml:m </mml:msub></mml:mrow></mml:math 	i>iQ<∕mm 3.4	l:mi> <mml:m< td=""></mml:m<>
168	Template-free synthesis of ternary sulfides submicrospheres as visible light photocatalysts by ultrasonic spray pyrolysis. Catalysis Science and Technology, 2012, 2, 1825.	4.1	22
169	Facile Synthesis of Visible-Light-Activated F-Doped TiO ₂ Hollow Spheres by Ultrasonic Spray Pyrolysis. Science of Advanced Materials, 2012, 4, 863-868.	0.7	10
170	Template-free fabrication and growth mechanism of uniform (BiO)2CO3 hierarchical hollow microspheres with outstanding photocatalytic activities under both UV and visible light irradiation. Journal of Materials Chemistry, 2011, 21, 12428.	6.7	142
171	Rose-like monodisperse bismuth subcarbonate hierarchical hollow microspheres: One-pot template-free fabrication and excellent visible light photocatalytic activity and photochemical stability for NO removal in indoor air. Journal of Hazardous Materials, 2011, 195, 346-354.	12.4	151
172	Application Research at the Nano and Advanced Materials Institute. IEEE Nanotechnology Magazine, 2011, 5, 13-22.	1.3	1
173	Efficient Visible Light Photocatalytic Removal of NO with BiOBr-Graphene Nanocomposites. Journal of Physical Chemistry C, 2011, 115, 25330-25337.	3.1	208
174	Photocatalytic removal of NO and HCHO over nanocrystalline Zn2SnO4 microcubes for indoor air purification. Journal of Hazardous Materials, 2010, 179, 141-150.	12.4	75
175	DRIFT Study of the SO ₂ Effect on Low-Temperature SCR Reaction over Feâ^'Mn/TiO ₂ . Journal of Physical Chemistry C, 2010, 114, 4961-4965.	3.1	232
176	Ultrasonic Spray Pyrolysis Synthesis of Porous Bi ₂ WO ₆ Microspheres and Their Visible-Light-Induced Photocatalytic Removal of NO. Journal of Physical Chemistry C, 2010, 114, 6342-6349.	3.1	195
177	Characterization of winter airborne particles at Emperor Qin's Terra-cotta Museum, China. Science of the Total Environment, 2009, 407, 5319-5327.	8.0	35
178	Biomolecule-controlled hydrothermal synthesis of C–N–S-tridoped TiO2 nanocrystalline photocatalysts for NO removal under simulated solar light irradiation. Journal of Hazardous Materials, 2009, 169, 77-87.	12.4	168
179	Aerosol-assisted flow synthesis of B-doped, Ni-doped and B–Ni-codoped TiO2 solid and hollow microspheres for photocatalytic removal of NO. Applied Catalysis B: Environmental, 2009, 89, 398-405.	20.2	102
180	Interfacial Hydrothermal Synthesis of Cu@Cu ₂ O Coreâ^'Shell Microspheres with Enhanced Visible-Light-Driven Photocatalytic Activity. Journal of Physical Chemistry C, 2009, 113, 20896-20902.	3.1	217

#	Article	IF	CITATIONS
181	Atmospheric deterioration of Qin brick in an environmental chamber at Emperor Qin's Terracotta Museum, China. Journal of Archaeological Science, 2009, 36, 2578-2583.	2.4	14
182	Growth-differentiation factor-8 (GDF-8) in the uterus: its identification and functional significance in the golden hamster. Reproductive Biology and Endocrinology, 2009, 7, 134.	3.3	9
183	Efficient Photocatalytic Removal of NO in Indoor Air with Hierarchical Bismuth Oxybromide Nanoplate Microspheres under Visible Light. Environmental Science & Technology, 2009, 43, 4143-4150.	10.0	426
184	Vehicular emission of volatile organic compounds (VOCs) from a tunnel study in Hong Kong. Atmospheric Chemistry and Physics, 2009, 9, 7491-7504.	4.9	143
185	Effect of Carbon Doping on the Mesoporous Structure of Nanocrystalline Titanium Dioxide and Its Solar-Light-Driven Photocatalytic Degradation of NO <i>_x</i> . Langmuir, 2008, 24, 3510-3516.	3.5	288
186	Gaseous and particulate polycyclic aromatic hydrocarbons (PAHs) emissions from commercial restaurants in Hong Kong. Journal of Environmental Monitoring, 2007, 9, 1402.	2.1	61
187	Photocatalytic activity and photo-induced hydrophilicity of mesoporous TiO2 thin films coated on aluminum substrate. Applied Catalysis B: Environmental, 2007, 73, 135-143.	20.2	40
188	Sonochemical synthesis and visible light photocatalytic behavior of CdSe and CdSe/TiO2 nanoparticles. Journal of Molecular Catalysis A, 2006, 247, 268-274.	4.8	146
189	Preparation, characterization and photocatalytic activity of in situ Fe-doped TiO2 thin films. Thin Solid Films, 2006, 496, 273-280.	1.8	154
190	Synthesis of hierarchical nanoporous F-doped TiO2 spheres with visible light photocatalytic activity. Chemical Communications, 2006, , 1115.	4.1	359
191	Low-temperature hydrothermal synthesis of S-doped TiO2 with visible light photocatalytic activity. Journal of Solid State Chemistry, 2006, 179, 1171-1176.	2.9	245
192	Efficient Visible-Light-Induced Photocatalytic Disinfection on Sulfur-Doped Nanocrystalline Titania. Environmental Science & Technology, 2005, 39, 1175-1179.	10.0	754
193	Photocatalytic TiO2/Glass Nanoflake Array Films. Langmuir, 2005, 21, 3486-3492.	3.5	41
194	Preparation and Photocatalytic Behavior of MoS2 and WS2 Nanocluster Sensitized TiO2. Langmuir, 2004, 20, 5865-5869.	3.5	519
195	Sono- and Photochemical Routes for the Formation of Highly Dispersed Gold Nanoclusters in Mesoporous Titania Films. Advanced Functional Materials, 2004, 14, 1178-1183.	14.9	83
196	Preparation of a highly active nanocrystalline TiO2 photocatalyst from titanium oxo cluster precursor. Journal of Solid State Chemistry, 2004, 177, 2584-2590.	2.9	50
197	A Simple and General Method for the Synthesis of Multicomponent Na2V6O16·3H2O Single-Crystal Nanobelts. Journal of the American Chemical Society, 2004, 126, 3422-3423.	13.7	158
198	Preparation and photocatalytic behavior of MoS2 and WS2 nanocluster sensitized TiO2. Langmuir, 2004, 20, 5865-9.	3.5	54

#	Article	IF	CITATIONS
199	Photocatalytic Activity, Antibacterial Effect, and Photoinduced Hydrophilicity of TiO2Films Coated on a Stainless Steel Substrate. Environmental Science & amp; Technology, 2003, 37, 2296-2301.	10.0	359
200	Effects of acidic and basic hydrolysis catalysts on the photocatalytic activity and microstructures of bimodal mesoporous titania. Journal of Catalysis, 2003, 217, 69-69.	6.2	518
201	Effects of alcohol content and calcination temperature on the textural properties of bimodally mesoporous titania. Applied Catalysis A: General, 2003, 255, 309-320.	4.3	117
202	The Effect of Calcination Temperature on the Surface Microstructure and Photocatalytic Activity of TiO2 Thin Films Prepared by Liquid Phase Deposition. Journal of Physical Chemistry B, 2003, 107, 13871-13879.	2.6	1,113
203	Effects of Trifluoroacetic Acid Modification on the Surface Microstructures and Photocatalytic Activity of Mesoporous TiO2Thin Films. Langmuir, 2003, 19, 3889-3896.	3.5	160
204	Effects of calcination temperature on the photocatalytic activity and photo-induced super-hydrophilicity of mesoporous TiO2 thin films. New Journal of Chemistry, 2002, 26, 607-613.	2.8	247
205	Enhancing effects of water content and ultrasonic irradiation on the photocatalytic activity of nano-sized TiO2 powders. Journal of Photochemistry and Photobiology A: Chemistry, 2002, 148, 263-271.	3.9	173
206	Light-induced super-hydrophilicity and photocatalytic activity of mesoporous TiO2 thin films. Journal of Photochemistry and Photobiology A: Chemistry, 2002, 148, 331-339.	3.9	131
207	Effects of F-Doping on the Photocatalytic Activity and Microstructures of Nanocrystalline TiO2Powders. Chemistry of Materials, 2002, 14, 3808-3816.	6.7	2,068
208	Preparation of highly photocatalytic active nano-sized TiO2 particles via ultrasonic irradiation. Chemical Communications, 2001, , 1942-1943.	4.1	321
209	Welcome to the new journal Photocatalysis. , 0, , .		0
210	Highly Efficient Photocatalytic Hydrogen Production Performance for 2D/0D g-C3N4/Zn0.5Cd0.5S with g-C3N4 as a Transport Medium for Photogenerated Charge Carriers. Journal of the Electrochemical Society, 0, , .	2.9	1